Accepted Manuscript

A label-free fluorescence biosensor for highly sensitive detection of lectin based on carboxymethyl chitosan-quantum dots and gold nanoparticles

Ziping Liu, Hua Liu, Lei Wang, Xingguang Su

PII: S0003-2670(16)30655-9

DOI: 10.1016/j.aca.2016.05.025

Reference: ACA 234591

To appear in: *Analytica Chimica Acta*

Received Date: 8 March 2016

Revised Date: 9 May 2016

Accepted Date: 12 May 2016

Please cite this article as: Z. Liu, H. Liu, L. Wang, X. Su, A label-free fluorescence biosensor for highly sensitive detection of lectin based on carboxymethyl chitosan-quantum dots and gold nanoparticles, *Analytica Chimica Acta* (2016), doi: 10.1016/j.aca.2016.05.025.

A label-free fluorescence biosensor for highly sensitive detection of lectin based on the integration of carboxymethyl chitosan, $CuInS_2$ quantum dots and gold nanoparticles

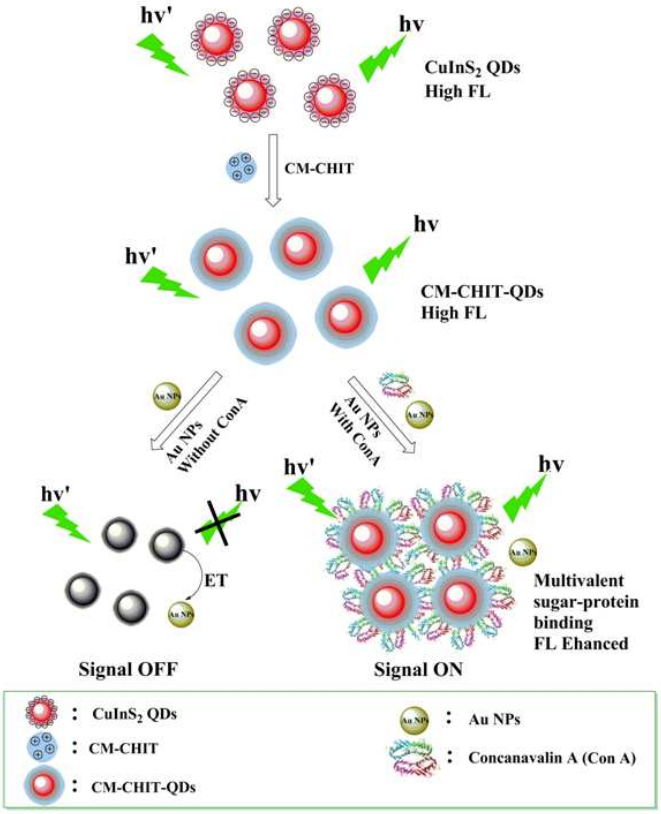

A label-free fluorescence biosensor for highly sensitive detection of lectin based on carboxymethyl chitosan-quantum dots and gold nanoparticles

Ziping Liu[a], Hua Liu[a], Lei Wang[a] and Xingguang Su[a*]

[a] *Department of Analytical Chemistry, College of Chemistry, Jilin University, Changchun 130012, P.R. China*

*Corresponding author

Tel.: +86-431-85168352

E-mail address: suxg@jlu.edu.cn

Abstract

In this work, we report a novel label-free fluorescence "turn off-on" biosensor for lectin detection. The highly sensitive and selective sensing system is based on the integration of carboxymethyl chitosan (CM-CHIT), $CuInS_2$ quantum dots (QDs) and Au nanoparticles (NPs). Firstly, $CuInS_2$ QDs featuring carboxyl groups were directly synthesized via a hydrothermal synthesis method. Then, the carboxyl groups on the $CuInS_2$ QDs surface were interacted with the amino groups ($-NH_2$), carboxyl groups (-COOH) and hydroxyl groups (-OH) within CM-CHIT polymeric chains via electrostatic interactions and hydrogen bonding to form CM-CHIT-QDs assemblies. Introduction of Au NPs could quench the fluorescence of CM-CHIT-QDs through electron and energy transfer. In the presence of lectin, lectin could bind exclusively with CM-CHIT-QDs by means of specific multivalent carbohydrate-protein interaction. Thus, the electron and energy transfer process between CM-CHIT-QDs and Au NPs was inhibited, and as a result, the fluorescence of CM-CHIT-QDs was effectively "turned on". Under the optimum conditions, there was a good linear relationship between the fluorescence intensity ratio I/I_0 (I and I_0 were the fluorescence intensity of CM-CHIT-QDs-Au NPs in the presence and absence of lectin, respectively) and lectin concentration in the range of 0.2-192.5 $nmol \cdot L^{-1}$, And the detection limit could be down to 0.08 $nmol \cdot L^{-1}$. Furthermore, the proposed biosensor was employed for the determination of lectin in fetal bovine serum samples with satisfactory results.

Keywords: Fluorescence biosensor; Lectins; $CuInS_2$ QDs; Au NPs; Carbohydrate-protein interactions

1. Introduction

Lectins are proteins or glycoproteins of nonimmune origin that come from plants, animals or microorganisms. They are capable of binding ability to mono/oligosaccharides as well as sugar residues in cell walls/membranes with a high degree of stereospecificity [1-2]. The specific carbohydrate-protein interactions mediate many important physiological and patho-physiological processes in living organism, such as bacterial and viral infections, cancer metastasis, inflammation, and immune surveillance [3]. Therefore, their study has attracted great attention due to their significance in understanding the important biological processes and in developing biosensors for clinical diagnostics and drug development.

Up to now, there are many assays for lectins quantification and/or detection because of their important functions including cell-cell interactions, homing of leukocytes, host pathogen interactions, biosynthesis and quality control of glycoproteins, malignancy and metastasis [4]. They also find applications in bioanalytical chemistry and molecular biology [5]. Assays for lectins based on the principle of carbohydrate-protein interaction are routinely realized by agglutination inhibition assays [6], enzyme-linked immunosorbent assay (ELISA) [7], colorimetry [8-9] or surface plasmon resonance (SPR) [10-11]. But most of these analytical methods are time-consuming, expensive, and must be manipulated by trained personnel. Moreover, the conventional approaches relying on the monovalent carbohydrate-protein interaction are generally weak and involve low sensitivity [12]. So far, great efforts have been devoted to overcome such shortcomings.

Recently, there are exciting findings that the weak carbohydrate-protein interactions can be effectively strengthened by presenting multiple ligands to their respective binding proteins [13-14]. Several works have proved that the resulting polyvalent interactions between the multiple ligands and proteins are much stronger than the corresponding monovalent carbohydrate-protein interactions [15-16]. However, tedious procedures for preparing the derivatives of carbohydrate,

complicated detection facilities, controlled storing conditions are involved in these methods, which severely restricted their extensive applications for sensitive and rapid lectin detection. In addition, many sensing systems required labeling procedures, which are usually laborious, cumbersome, and error-prone [17]. Thus far, developing fast, facile, label-free, cost-effective glycotechnologies and biosensors with high sensitivity for lectins detection still remains a great challenge.

For high-throughput and easy operation homogeneous detection of proteins, QDs-based assays are promising alternatives to circumvent some of the functional limitations encountered by protein arrays and suspension arrays due to their unique electro-optical properties and photophysical features, like high quantum yields, long fluorescence lifetimes, higher brightness and stability against photobleaching, broad absorption spectra coupled with narrow photoluminescent emission spectra [18-19]. Currently, QDs integrated with biomolecules have attracted great interest for advanced biological applications in biosensing, medical diagnostics, cell imaging, and gene delivery [20-21]. But the applications of QDs to the clinical field have been hampered owing to their high toxicity. Regular QDs-based reports are focused on the cadmium-based QDs that are toxic to biological systems, chemical and photochemical disturbances, and eventually would cause serious environmental problems due to the leakage of cadmium [22].

With regard to this, two main approaches have been employed to reduce the toxicity of QDs. One is to cover non-toxic substance, such as silica shell, and the other is to develop novel QDs without heavy metal ions. In recent years, the newly emerging I-III-VI $CuInS_2$ QDs are particularly impressive because they do not contain any toxic class A elements (Cd, Pb, and Hg) or class B elements (Se and As) [23-24]. Moreover, $CuInS_2$ QDs are near-infrared region (NIR) QDs

(generally wavelengths＞650 nm), and can operate in the NIR and avoid interference from biological media, mainly tissue autofluorescence and scattering light [25]. Despite of great explorations of NIR fluorescence sensors in the field of biological imaging, the NIR fluorescence sensors for the determination of complex analytes, such as protein molecules, are still a highly desirable research objective [26].

Herein, we report a facile near-infrared label-free fluorescence “turn off-on” biosensor for lectin detection based on the integration of CM-CHIT, $CuInS_2$ QDs and Au NPs. Concanavalin A (Con A), widely exploited for studying carbohydrate-lectins interactions, is chosen as a modle lectin to demonstrate proof-of-concept of the methodology. Con A exists as a tetramer at neutral pH and binds exclusively with α-glucose, α-mannose and their derivatives containing mannose and glucose residues [27,28]. CM-CHIT, a water soluble chitosan derivative, is composed of N-acetyl-glucosamine that can specifically recognize Con A by means of specific carbohydrate-ConA interaction. Noteworthy, the amino groups ($-NH_2$), carboxyl groups (-COOH) and hydroxyl groups (-OH) within CM-CHIT chains can serve as electrostatic interaction and hydrogen bonding sites [29]. In addition, CM-CHIT also possesses many attractive physical and biological characteristics, such as high hydrophilic, low toxicity, good biocompatibility and biodegradability, which facilitate CM-CHIT a promising modification material [30-31]. Integration of Au NPs can significantly quench the fluorescence of CM-CHIT-QDs through electron transfer and energy transfer between CM-CHIT-QDs and Au NPs. Electron transfer and energy transfer can be inhibited by specific protein-carbohydrate interaction between CM-CHIT-QDs and ConA, and the quenched florescence of CM-CHIT-QDs is greatly recovered in the presence of ConA. To the best of our knowledge, this label-free and Au NPs

quenching-based lectins assay using CM-CHIT-QDs was developed for the first time.

2. Experimental section

2.1 Materials and apparatus

All chemicals and reagents were of at least analytical reagent grade and used as-received without any further purification. Copper (II) chloride dehydrate ($CuCl_2 \cdot 2H_2O$), indium (III) chloride tetrahydrate ($InCl_3 \cdot 4H_2O$), sulfourea (CS $(NH_2)_2$), mercaptopropionic acid (MPA), Con A, acid phosphatase (ACP), adenosine-5'-triphosphate (ATP), trypsin (Try) and carboxypeptidase Y (CPY) were purchased from Sigma-Aldrich Corporation. Chloroauric acid ($HAuCl_4$) was purchased from Acros Organics. Bovine serum albumin (BSA), pepsin (Pep) and human serum albumin (HSA) were obtained from Sino-American Biotechnology Co. Ltd. Lysozyme (Lyz) was purchased from Genview. Heparinase (Hep) was purchased from Si Qing Yuan Biotechnology (Beijing). CM-CHIT, sodium hydroxide (NaOH), sodium dehydrogenized phosphate (NaH_2PO_4), disodium hydrogen phosphate (Na_2HPO_4), sodium phosphate (Na_3PO_4) and the other chemicals used were all purchased from Beijing Dingguo Changsheng Biotechnology Co. Ltd. The water used in all experiments had a resistivity higher than 18 $M\Omega \cdot cm^{-1}$.

All the fluorescence measurements were performed on a Shimadzu RF-5301 PC spectrofluorophotometer (Shimadzu Co., Kyoto, Japan) equipped with a xenon lamp using right-angle geometry. A 1 cm path-length quartz cuvette was used in all experiments. The hydro-thermal synthesis experiments were accomplished in a JCZ-JL intelligent digital display drum wind drying oven. The ultrasonic processes was proceeded on a KQ2200 ultrasonic cleaner (Ultrasonic instrument Co., Kunshan, China). All pH measurements were completeed on a

PHS-3C pH meter (Tuopu Co., Hangzhou, China). The shaking processes were performed on a HY-2 variable-speed reciprocal shaker (Guo Hua Electric Appliance Co., Changzhou, China). The centrifugation processes were performed on a TGL-16G (Anke Technology Instrument Co., Shanghai, China). UV-vis absorption spectra were obtained using a Varian GBC Cintra 10e UV-vis spectrometer. Transmission electron microscopy (TEM) experiments were performed on a Philips Tecnai F20 TEM operating at 200 kV. Circular dichroism spectroscopic measurement were performed on a MOS-450 spectrometer connected with a peltier which controlled the temperature.

2.2 Preparation of CM-CHIT-$CuInS_2$ QDs

$CuInS_2$ QDs featuring carboxy groups were directly synthesized in aqueous solution via a hydrothermal synthesis method described in our previous report [32]. In a typical experiment, $CuCl_2 \cdot 2H_2O$ (0.15 mmol) and $InCl_3 \cdot 4H_2O$ (0.15 mmol) were dissolved in distilled water (7.5 mL). Then, MPA (1.80 mmol) was injected into the above solution. The pH of the mixture was adjusted to 11.3 by adding 4 $mol \cdot L^{-1}$ NaOH solution. 10 min later, CS $(NH_2)_2$ (0.30 mmol) was added into the solution. The Cu-to-In-to-S and Cu-to-MPA precursor ratios were 1:1:2 and 1:12, respectively. All the above mentioned experimental procedures were performed at room temperature. Then, the solution was transferred into a 15 mL Teflon-lined stainless steel autoclave. The autoclave was kept at 150℃ for 23 h and then cooled down to room temperature. The final concentration of $CuInS_2$ QDs was 1.36×10^{-4} $mol \cdot L^{-1}$.

The resulting QDs (1.36×10^{-4} $mol \cdot L^{-1}$, 3 mL) were added into CM-CHIT stock solution (5 $g \cdot L^{-1}$, 10 mL). The mixed solution was placed in an ultrasonic bath for 10 min, and then incubated overnight in dark with vibrating at room temperature. The excessive CM-CHIT was removed through the centrifugal separation. The final concentration of CM-CHIT-QDs was 3.14×10^{-5}

mol·L^{-1} QDs to 3.85 g·L^{-1} chitosan.

2.3 Synthesis of Au NPs

Au NPs were synthesized by the citrate reduction of $HAuC1_4$ according to the previous reports [33]. In a typical experiment, 1 mL $HAuCl_4$ solution (1%, V/V) and 99 mL deionized water were added into a 250 mL round-bottom three-necked flask. Then, the solution was heated to a boiling state under reflux condenser conditions with vigorous stirring. Subsequently, 5 mL trisodium citrate solution (1%) was quickly injected to the flask. When the color of the solution changed from pale yellow to deep red, the reaction was finished. The solution was cooled down to room temperature and then stored at 4 □ in the refrigerator for further use. The concentration of the Au NPs was 4 nmol·L^{-1}.

2.4. Fluorescence quenching experiments

For fluorescence quenching experiment, 200 μL CM-CHIT-QDs and a series of different amounts of Au NPs solution (from 0 to 400 μL) were separately mixed in 2.0 mL calibrated test tubes. Next, the mixed solutions were diluted to 1.5 mL with phosphate buffer solution and mixed thoroughly. 10 min later, the fluorescence spectra of CM-CHIT-QDs/Au NPs system were recorded in the 610-800 nm emission wavelength range at an excitation wavelength of 590 nm.

2.5. Fluorescence measurement of Con A

For Con A measurement, 200 μL CM-CHIT-QDs were successively placed in a series of 2.0 mL calibrated test tubes, respectively. Next, a series of different concentrations of Con A were added into the above mixtures and mixed thoroughly. 45 min later, 400 μL Au NPs were separately added into the solution and mixed thoroughly. Then, the mixed solutions were diluted to 1.5 mL with phosphate buffer solution and mixed thoroughly. At an excitation wavelength of 590 nm, the

fluorescence spectra of CM-CHIT-QDs/Au NPs system were recorded in the 610-800 nm emission wavelength range.

2.6. Circular dichroism spectroscopy measurements

Circular dichroism spectroscopic measurement of Con A before and after the conjugation of CM-CHIT-QDs/Au NPs was done on a MOS-450 spectrometer connected with a peltier which controlled the temperature. Con A samples (190 nM) were placed in a rectangular quartz cuvette with 1 mm path length, and the final concentration of CM-CHIT-QDs was 3.14×10^{-5} mol·L^{-1} QDs to 3.85 g·L^{-1} CM-CHIT. The concentration of Au NPs is 3.2 nM. The spectra were recorded at a scan speed of 20 nm/min with a response time of 4 s and slit width of 2 nm. Spectra were recorded both in far-UV (250-200 nm) and near-UV (320-250 nm) region. All measurements were conducted in 20 mM PBS (7.4 pH).

2.7. Detection of Con A in the fetal bovine serum samples

The fresh 10% fetal bovine serum was supplied by a local biological laboratory. The fetal bovine serum samples were diluted 100 times with PBS before detection. Different concentrations of Con A were added to the diluted fetal bovine serum samples to prepare the spiked samples. Dilution is a commonly adopted pretreatment procedure for Con A detection in a sample of high complexity. Detection processes were carried out under the optimized conditions.

3. Results and discussion

3.1 The strategy for the detection of Con A

As shown in Scheme 1, negatively charged quantum dots $CuInS_2$ QDs (featuring carboxyl groups) were firstly interacted with the amino groups (-NH_2), carboxyl groups (-COOH) and

hydroxyl groups (-OH) within CM-CHIT polymeric chains via electrostatic interactions and hydrogen bonding to form CM-CHIT-QDs assemblies. The as-prepared $CuInS_2$ QDs and CM-CHIT-QDs were characterized by using the transmission electron microscopy (TEM), UV-Vis absorption spectra, fluorescence emission spectra, and FT-IR spectroscopy. From the TEM images (Fig. S1-A), it can be seen that the $CuInS_2$ QDs were spherical particles and well dispersible in solution with diameters about 3-5 nm. After adding CM-CHIT, it can be obviously observed from Fig. S1-B that the size of the resulting CM-CHIT-QDs increased to about 10 nm. From Fig. 1, it could be observed that CM-CHIT-QDs emitted strong fluorescence with the maximal emission wavelength at 656 nm, and showed the maximum absorption at 590 nm (solid lines), which was consistent with that of $CuInS_2$ QDs (dash lines) [32]. Fig. 2 was the FT-IR spectra of the CM-CHIT-QDs and MPA capped $CuInS_2$ QDs. As shown in Fig. 2 (red curve), the majority of MPA functional groups could be clearly found through the characteristic peaks of -COOH (1560 cm^{-1} asymmetric stretching vibration, 1470 cm^{-1} symmetric stretching vibration), and the C-H stretching mode (2850 cm^{-1}, 2920 cm^{-1}, 2960 cm^{-1}). The characteristic peak of S-H did not appear within 2550-2680 cm^{-1}, which might be result from the covalent bonds between thiols and metal atoms of the $CuInS_2$ QDs [26]. We could ascertain that the original $CuInS_2$ QDs were capped by MPA. From the FT-IR spectra of CM-CHIT-QDs (green curve in Fig. 2), we could see that the characteristic C=O stretching peak (1730 cm^{-1}), -NH peaks (3400 cm^{-1}), C-O peak (1220 cm^{-1}) and $-CH_2$ (2850 cm^{-1} symmetric stretching vibration) appeared or enhanced, which indicated that the -COOH groups on the surface of $CuInS_2$ QDs had successfully reacted with the amino groups ($-NH_2$), carboxyl groups (-COOH) and hydroxyl groups (-OH) within CM-CHIT.

When Au NPs is introduced, Au NPs could quench the fluorescence of CM-CHIT-QDs via

electron transfer and energy transfer process. Compared to organic quenchers, nanomaterial quenchers possess excellent properties of high stability, superquenching efficiency and biocompatibility. However, in the presence of Con A, Con A could bind to CM-CHIT-QDs through exclusively multivalent sugar-protein interactions. Therefore, the electron transfer and energy transfer process between CM-CHIT-QDs and Au NPs was hindered, and as a result the fluorescence of CM-CHIT-QDs was greatly activated to a “turn-on” state. Thus, the determination of lectin could be achieved by monitoring the fluorescence “turn off-on”.

3.2 Resonance light scattering and circular dichroism spectroscopy measurement

To validate the feasibility of the strategy, the resonance light scattering (RLS) technique was used in this study. Fig. 3 was the RLS spectra of CM-CHIT-QDs, CM-CHIT-QDs/Au NPs, CM-CHIT-QDs/Au NPs/Con A, Con A and Au NPs system. From Fig. 3, it could be seen that Au NPs showed only one RLS peak at 590 nm in the wavelength region of 450-800 nm. Con A showed three RLS peaks at 548 nm, 563 nm and 643 nm, respectively. CM-CHIT-QDs solution showed four RLS peaks at 548 nm, 563 nm, 623 nm and 637 nm, respectively. CM-CHIT-QDs/Au NPs without Con A had three RLS peaks at 548 nm, 563 nm and 623 nm, respectively. When CM-CHIT-QDs/Au NPs was incubated with Con A, the scattering intensities at 548 nm, 563 nm, 590 nm and 623 nm were apparently enhanced, which indicates the diameter of particles in the presence of Con A was much larger than that in the absence of Con A. The main reason for the RLS intensity enhancement was owing to the carbohydrate-protein interaction between CM-CHIT-QDs and Con A, which could form CM-CHIT-QDs/Au NPs/Con A complex.

The CD spectra of Con A before and after the conjugation of CM-CHIT-QDs/Au NPs was further studied. As seen in Fig. 3B, the CD spectra of Con A showed a negative band at 230 nm

and positive bands at 206 nm and 249-290 nm, indicating that this protein consisted essentially of a mixture of β-form and random coil, and aromatic amino acid residues existed [34]. After the conjugation of CM-CHIT-QDs/Au NPs, the CD bands of Con A at both the negative band (230 nm) and positive bands (206 nm and 249-290 nm) reduced, suggesting the interactions between Con A and CM-CHIT-QDs/Au NPs would result in a decrease of the β-form and random coil content to some extent [35].

3.3 Quenching effects of Au NPs on the fluorescence of CM-CHIT-QDs

According to the previous reports, semiconductor QDs were proven to be very effective fluorescence resonance energy transfer donors, and several fluorescence resonance energy transfer based biosensing system utilizing QDs have been demonstrated in the past few years [36,37]. Conversely, Au NPs are known for their capacity to quench the fluorescence of semiconductor QDs as the efficient energy acceptors [38,39]. In the present work, CM-CHIT-QDs were mixed with different amounts of Au NPs, and the fluorescence intensity changes of the CM-CHIT-QDs were monitored (Fig. 4). As expected, the fluorescence intensity of the CM-CHIT-QDs at 656 nm gradually decreased with the increasing concentration of Au NPs (from 0 to 3.2 nmol·L^{-1}) (as seen in Fig. 4). The inset showed the relationship between the fluorescence quenching ratios I/I_0 and the concentration of Au NPs. I and I_0 were the fluorescence intensity of CM-CHIT-QDs in the presence and absence of Au NPs, respectively. There was good linearity between I/I_0 and Au NPs in the concentration range of 0.053 to 3.2 nmol·L^{-1}. The regression equation was I/I_0=0.991-0.196 [Au NPs], nmol·L^{-1}. The corresponding regression coefficient was 0.986. Finally, 1.0×10^{-9} mol·L^{-1} Au NPs was used in the further experiments.

The energy transfer efficiency between QDs and Au NPs depends on several factors such as the

particle size and shape as well as the separation distance between the donor and the gold quencher [40,41]. Wu's group had discussed in detail about the effect of three different sized Au NPs (3, 15, and 80 nm), which had different localized surface plasmon resonance absorption band, on the energy transfer between the CdSe/ZnS QDs and the Au NPs [42]. The 3 nm sized Au NPs have negligible localized surface plasmon resonance absorption and quench the fluorescence emission of the QDs with a $1/d^4$ distance-dependence, indicating the nanometal surface energy transfer mechanism. The 15 and 80 nm sized Au NPs have strong localized surface plasmon resonance absorption bands that overlap with the emission band of the QDs. The energy transfer efficiency depends on the $1/d^6$ separation distance, which is dominated by the dipole-dipole interaction according to Förster resonance energy transfer. The 80 nm sized Au NPs displays higher quenching efficiency due to the increased spectral overlap of the localized surface plasmon resonance absorption band with the emission band of QDs. From the TEM images of Au NPs used in this work (Fig. S1-C), it could be seen that the shapes of Au NPs were monodisperse, and spherical, and the average size was about 13.1 nm in diameter. Figure S2 was the normalized extinction spectra of Au NPs and normalized fluorescence emission spectra of CM-CHIT-QDs. From Figure S2, it can be observed that the fluorescence emission band of the QDs exhibited partial spectral overlap with the localized surface plasmon resonance band of the Au NPs, which is consistent with the previous reports [42]. All the above results confirm that Au NPs could quench the fluorescence of CM-CHIT-QDs via electron transfer and energy transfer process.

3.4 Optimization for Con A detection

In order to achieve better sensing performance for Con A, experimental parameters, such as the concentration of CM-CHIT, pH, salt concentration and reaction time were optimized. The effect of

the CM-CHIT concentration in the range of 0 to 5.0 $g \cdot L^{-1}$ was firstly investigated (as seen in Fig. 5A). It is known that a large concentration CM-CHIT is beneficial to the carbohydrate-protein interactions between CM-CHIT and Con A. However, large concentration of CM-CHIT would lead to the fluorescence of CM-CHIT-QDs decrease (as shown in Fig. 5A). Therefore, a final concentration of 3.85 $g \cdot L^{-1}$ CM-CHIT was adopted for the sensor preparation to achieve little fluorescence decrease and maximum sensitivity.

The effect of pH was studied over the range of 5.0 - 9.0 (Fig. 5B). It can be observed from Fig. 5B that the fluorescence intensity ratio I/I_0 (I and I_0 are the fluorescence intensity of CM-CHIT-QDs/Au NPs in the presence and absence of Con A, respectively) increased gradually from pH 5.0 to 7.4, and then decreased when the pH was over 7.4. According to the previous literatures, Con A exists as a single dimer below pH 5.6 and exists predominantly as a tetramer of four identical subunits at neutral and alkaline pH [43-44]. Significantly, divalent cations must be present to permit the binding of Con A to carbohydrates because they are necessary in order to get an active Con A conformation [45]. At low pH, Con A would release metal ions and exist in inactive diametric form, which further weakened the carbohydrate-protein interactions between CM-CHIT-QDs and Con A and led to significant fluorescence intensity ratio I/I_0 decrease. High pH would cause the denaturation of ConA, which thereby led to low binding affinity of ConA towards CM-CHIT-QDs and subsequent the decrease of fluorescence intensity ratio I/I_0. Hence, a pH 7.4 PBS containing $MnCl_2$ (0.1 mM) and $CaCl_2$ (0.1 mM) was selected for the further experiment. The effect of salt concentration on the fluorescence intensity of Au NPs/CM-CHIT-QDs system in the absence and presence of Con A was also studied. From Fig. 5C, we could see that the salt concentration had no significant influence on the fluorescence intensity

of the Au NPs/CM-CHIT-QDs/Con A system. So, 10 μmol·L^{-1} NaCl was chosen in this work.

Then, the effect of incubation time on the fluorescence intensity of CM-CHIT-QDs in the presence of Au NPs was studied. As shown in Fig. 5D, the fluorescence intensity decreased sharply in the first 2 min of incubation time, and then decreased gradually with the increasing of incubation time until 12 min, which indicated the quenching effect of Au NPs on the fluorescence of CM-CHIT-QDs was completed within 12 min. Therefore, the fluorescence intensity of the CM-CHIT-QDs/Au NPs system was recorded after incubation of 12 min. The effect of incubation time on the fluorescence intensity of CM-CHIT-QDs/Au NPs in the presence of Con A was further investigated. As shown in Fig. 5E, the fluorescence intensity gradually increased with the increasing of incubation time until 45 min, which indicated the fluorescence recovery finished within 45 min. So we recorded the fluorescence intensity of the CM-CHIT-QDs/Au NPs/Con A system after incubation of 45 min.

3.5 Fluorescence "turn on" detection of Con A

Under the optimized conditions, a systematic study was carried out to investigate whether the proposed fluorescence biosensor could quantitatively detect Con A. As shown in Fig. 6A, the fluorescence intensity of CM-CHIT-QDs/Au NPs increased gradually with the increasing concentration of Con A in the range of 0-302.5 nmol·L^{-1}. Fig. 6A inset illustrated there was good linearity between the fluorescence intensity ratio I/I_0 (I and I_0 were the fluorescence intensity of CM-CHIT-QDs/Au NPs in the presence and absence of Con A, respectively) and Con A concentration in the range of 0.2-192.5 nmol·L^{-1}. The regression equation was I/I_0=1.170-0.0120 [Con A], nmol·L^{-1}. The corresponding regression coefficient (R^2) was 0.999. The detection limit (LOD) was down to 0.08 nmol·L^{-1}. The detection limit is defined by the equation LOD=3σ/s,

where σ is the standard deviation of the blank signals and s is the slope of the calibration curve. Compared with conventional other methods, our method for Con A shows a reasonably good Con A quantification range and a lower LOD. Moreover, the Au NPs-modulated CM-CHIT-QDs-based fluorescence "turn off-on" biosensor is a novel sensing system with the advantages of superior sensitivity, costeffective design and a facile fabrication process.

In addition, we also studied the interaction between CM-CHIT-QDs and Con A (as shown in Fig.7). The results were shown in Fig. 6B. From Fig. 6B, it could be seen that the fluorescence intensity of CM-CHIT-QDs increased gradually with the increasing concentration of Con A in the range of 0-120 nmol·L^{-1}. The inset in Fig. 6B illustrated that there was a linear relationship between the fluorescence intensity ratio I/I_0 (I and I_0 were the FL intensities of CM-CHIT-QDs in the presence and absence of Con A, respectively) and Con A concentration in the range of 2.5-45 nmol·L^{-1}. The regression equation was I/I_0= 0.980-0.008 [Con A], nmol·L^{-1}. The corresponding regression coefficient (R^2) was 0.988. The detection limit (LOD) was 0.99 nmol·L^{-1}. Compared with the CM-CHIT-QDs system for Con A detection, the CM-CHIT-QDs/Au NPs system had the lower detection limit. The higher sensitivity was supposed to due to the integration of Au NPs, which reduced the background fluorescence and ultimately led to highly sensitive detection of ConA.

3.6 Interference study

Selectivity is a very important parameter to evaluate the performance of a new sensor, especially for a biosensor with potential applications in biomedical samples, a highly selective response to the target over other potentially coexisting species is necessary. Therefore, the selectivity experiments for our proposed biosensor were carried out with various coexisting

substances added. Fig. S3 is the fluorescence spectra of CM-CHIT-QDs/Au NPs/Con A system in the absence and presence of coexisting substances, respectively. Table 1 showed the interference effect of inorganic ions and some biological important molecules on the determination of Con A, a relative error of ±5.0% was considered to be tolerable. As shown in Table 1, the tolerable concentration ratios of coexisting substances to 1 nmol·L^{-1} Con A was over 1000 fold for Na^+, K^+, Cl^-, NO^{3-} and SO_4^{2-}, 500 fold for glucose, fructose and galactose, 100 fold for bovine serum albumin (BSA), human serum albumin (HAS), heparinase (Hep) and lysozyme (Lyz). These results demonstrated that the novel sensor displays high selectivity for the determination of Con A.

3.7 Detection of Con A in fetal bovine serum samples

In order to testify the accuracy and precision of the proposed method, it was applied for the detection of Con A in the fetal bovine serum samples. The concentration of Con A in the fetal bovine serum samples was determined by the standard addition method and the results were listed in Table 2. From Table 2, we can see that the RSD was lower than 3.5% and the average recoveries of Con A in the fetal bovine serum samples were in the range of 97-101%. The above results indicated that the accuracy and precision of the present method is satisfied.

4. Conclusion

In summary, a label-free, low-cost biosensor has been successfully developed to detect Con A on the basis of CM-CHIT-QDs and Au NPs. Although CM-CHIT-QDs can bind specifically to Con A with high selectivity over noncognate proteins, it is not enough sensitively sensing due to the high fluorescence background signals. By taking advantage of the fluorescence quenching

capability of Au NPs, the background fluorescence is low, which ultimately leads to highly sensitive detection of ConA. Noteworthy, the detection limit could be down to 0.08 nmol·L^{-1}. This nano-biosensor was proved to be rapid, convenient and tolerance of most interfering substances. Furthermore, the proposed biosensor was employed for the determination of lectin in fetal bovine serum samples with satisfactory results. Given the advantages arising from the combination of biosensor design and novel nanomaterials, we expect this assay could form a generic platform for advanced biomolecular sensing with a high promise in practical applications.

Acknowledgement

This work was financially supported by the National Natural Science Foundation of China (Nos. 21075050 and 21275063), the Science and Technology Development project of Jilin province, China (No. 20150204010GX).

References

[1] H. Lis and N. Sharon, Lectins: carbohydrate-specific proteins that mediate cellular recognition, *Chem. Rev.*, 98 (1998) 637-674.

[2] X.-P. He, X.-W. Wang, X.-P. Jin, H. Zhou, X.-X. Shi, G.-R. Chen, Y.-T. Long, Epimeric monosaccharide-quinone hybrids on gold electrodes toward the electrochemical probing of specific carbohydrate-protein recognitions. *J. Am. Chem. Soc.* 133 (2011) 3649-3657.

[3] N. Sharon, H. Lis, Lectins as cell recognition molecules, *Science* 246 (1989) 227-234.

[4] M. Mammen, S.-K. Choi and G. M. Whitesides, Polyvalent interactions in biological systems: implications for design and use of multivalent ligands and inhibitors, *Angew. Chem., Int. Ed.* 37 (1998) 2754-2794.

[5] J. B. Lowe and J. D. Marth, The biochemistry of plant lectins (phytohemagglutinins), *Annu. ReV. Biochem.* 72 (2003) 643-691.

[6] R. Carrotta, S. Vilasi, F. Librizzi, V. Martorana, D. Bulone, P. L. San Biagio, α-Casein inhibition mechanism in concanavalin A aggregation process, *J. Phys. Chem. B* 116 (2012) 14700-14707.

[7] Y. Kamada, N. Kinoshita, Y. Tsuchiya, K. Kobayashi, H. Fujii, N. Terao, K. Kamihagi, N. Koyama, S. Yamada, Y. Daigo, Y. Nakamura, N. Taniguchi, E. Miyoshi, Reevaluation of a lectin antibody ELISA kit for measuring fucosylated haptoglobin in various conditions, *Clin. Chim. Acta* 417 (2013) 48-53.

[8] C. S. Tsai, T. B. Yu, C. T. Chen, Gold nanoparticle-based competitive colorimetric assay for detection of protein-protein interactions, *Chem. Commun.* 2005, 4273-4275.

[9] X.-L. Hu, H.-Y. Jin, X.-P. He, T. D. James, G.-R. Chen and Y.-T. Long, Colorimetric and plasmonic detection of lectins using core-shell gold glyconanoparticles prepared by copper-free click chemistry, *ACS Appl. Mater. Interfaces*, 7 (2015) 1874-1878.

[10] C. Jimé nez-Castells, S. Defaus, A. Moise, M. Przbylski, D. Andreu, R. Gutié rrez-Gallego, Surface-based and mass spectrometric approaches to deciphering sugar-protein interactions in a galactose-specific agglutinin. *Anal. Chem.* 84 (2012) 6515-6520.

[11] C.-F. Huang, G.-H. Yao, R.-P. Liang, J.-D. Qiu, Graphene oxide and dextran capped gold

nanoparticles based surface plasmon resonance sensor for sensitive detection of concanavalin A, *Biosensors and Bioelectronics*, 50 (2013) 305-310.

[12] R. J. Pieters, Maximising multivalency effects in protein-carbohydrate interactions, *Org. Biomol. Chem*. 7 (2009) 2013-2025.

[13] R. Jelinek, S. Kolusheva, Carbohydrate biosensors, *Chem. Rev.* 104 (2004) 5987-6016.

[14] J. M. de la Fuente, P. Eaton, A. G. Barrientos, M. Menéndez, S. J. Penadés, Thermodynamic evidence for Ca^{2+}-mediated self-aggregation of lewis X gold glyconanoparticles. a model for cell adhesion via carbohydrate-carbohydrate interaction, *Am. Chem. Soc*. 127 (2005) 6192-6197.

[15] L. H. Wang, K.-Y. Pu, J. Li, X. Y. Qi, H. Li, H. Zhang, C. H. Fan and B. Liu, A graphene-conjugated oligomer hybrid probe for light-up sensing of lectin and *escherichia coli*, *Adv. Mater.* 23 (2011) 4386-4391.

[16] H. Vedala, Y. Chen, S. Cecioni, A. Imberty, S. Vidal, A. Star, Nanoelectronic detection of lectin-carbohydrate interactions using carbon nanotubes, *Nano Lett.* 11 (2011) 170-175.

[17] O. A. Loaiza, P. J. L.-Ardisana, E. Jubete, E. Ochoteco, I. Loinaz, G. an Cabanero, I. García, and Soledad Penades, Nanostructured disposable impedimetric sensors as tools for specific biomolecular interactions: sensitive recognition of concanavalin A, *Anal. Chem.* 83 (2011) 2987-2995.

[18] R. Freeman, I. Willner, Optical molecular sensing with semiconductor quantum dots (QDs), *Chem. Soc. Rev.* 41 (2012) 4067-4085.

[19] X. Gao, J. Wu, X. Wei, C. He, X. Wang, G. Guo, Q. Pu, Facile one-step photochemical synthesis of water soluble CdTe(S) nanocrystals with high quantum yields, *J. Mater. Chem.* 22 (2012) 6367-6373.

[20] J. K. Jaiswal, S. M. Simon, Potentials and pitfalls of fluorescent quantum dots for biological imaging, *Trends Cell Biol.* 14 (2004) 497-504.

[21] X. Michalet, F. F. Pinaud, L. A. Bentolila, J. M. Tsay, S. Doose, J. J. Li, G. Sundaresan, A. M. Wu, S. S. Gambhir, S. Weiss, Quantum dots for live cells, in vivo imaging, and diagnostics, *Science* 307 (2005) 538-544.

[22] R. Hardman, A toxicologic review of quantum dots: toxicity depends on physicochemical and environmental factors, *Environ. Health Persp.* 114 (2006) 165-172.

[23] R. G. Xie, M. Rutherford, X. G. Peng, Formation of high-quality I-III-VI semiconductor nanocrystals by tuning relative reactivity of cationic precursors, *J. Am. Chem. Soc*. 131 (2009) 5691-5697.

[24] H. Nakamura, W. Kato, M. Uehara, K. Nose, T. Omata, S. O. Y. Matsuo, M. Miyazaki, H. Maeda, Tunable photoluminescence wavelength of chalcopyrite $CuInS_2$-based semiconductor nanocrystals synthesized in a colloidal system, *Chem. Mater*. 18 (2006) 3330-3335.

[25] Z. H. Lin, Q. Ma, X. F. Fei, H. Zhang, X. G. Su, A novel aptamer functionalized $CuInS_2$ quantum dots probe for daunorubicin sensing and near infrared imaging of prostate cancer cells. *Analytica Chimica Acta* 818 (2014) 54-60.

[26] S.Y. Liu, F. P. Shi, X. J. Zhao, L. Chen, X. G. Su, 3-Aminophenyl boronic acid-functionalized $CuInS_2$ quantum dots as a near-infrared fluorescence probe for the determination of dopamine, *Biosens. Bioelectron.* 47 (2013) 379-384.

[27] A. Samanta, M. C. A. Stuart, B. J. Ravoo, Photoresponsive capture and release of lectins in multilamellar complexes. *J. Am. Chem. Soc.* 134 (2012) 19909-19914.

[28] Y. Gou, S. Slavin, J. Geng, L. Voorhaar, D. M. Haddleton, C. R. Becer, Controlled alternate layer-by-layer assembly of lectins and glycopolymers using QCM-D, *ACS Macro Lett.* 1 (2012) 180-183.

[29] X. Zeng, E. Ruckenstein, Membrane chromatography: Preparation and applications to protein separation, *Biotechnol. Prog.* 15 (1999) 1003-1019.

[30] X. Chen, Z. Wang, W. Liu, H. Park, The effect of carboxymethyl-chitosan on proliferation and collagen secretion of normal and keloid skin fibroblasts, *Biomaterials* 23 (2002) 4609-4614.

[31] A. Zhu, N. Fang, Adhesion dynamics, morphology, and organization of 3T3 fibroblast on chitosan and its derivative: The effect of O-carboxymethylation, *Biomacromolecules* 6 (2005) 2607-2614.

[32] S. Y. Liu, H. Zhang, Y. Qiao, X. G. Su, One-pot synthesis of ternary $CuInS_2$ quantum dots with near-infrared fluorescence in aqueous solution, *RSC Advances*. 2 (2012) 819-825.

[33] F. Gao, P. Cui, X. Chen, Q. Ye, M. Li, L. Wang, Efficient fluorescence energy transfer system between CdTe-doped silica nanoparticles and gold nanoparticles for turn-on fluorescence detection of melamine, *Analyst* 136 (2011) 3973-3980.

[34] D. William, McCubbin, O. Kimio, M. K. Cyril, Circular dichroism studies on concanavalin A, 1971, 43, 666-674.

[35] D.William, McCubbin, O. Kimio, M. K. Cyril, Circular dichroism studies on chemically modified derivatives of concanavalin A, 1972, 23, 100-104.

[36] I. L. Medintz, H. T. Uyeda, E. R. Goldman, H. Mattoussi, Quantum dot bioconjugates for imaging, labelling and sensing, *Nat. Mater.* 4 (2005) 435-446.

[37] X. Michalet, F. F. Pinaud, L. A. Bentolila, J. M. Tsay, S. Doose, J. J. Li, G. Sundaresan, A. M. Wu, S. S. Gambhir, S. Weiss, Quantum dots for live cells, in vivo imaging, and diagnostics, *Science* 307 (2005) 538-544.

[38] T. Pons, I. L. Medintz, K. E. Sapsford, S. Higashiya, A. F. Grimes, On the quenching of semiconductor quantum dot photoluminescence by proximal gold nanoparticles, *Nano Lett.* 7 (2007) 3157-3164.

[39] Y. Li, Q. Ma, Z. P. Liu, X. Y. Wang, X. G. Su, A novel enzyme-mimic nanosensor based on quantum dot-Au nanoparticle@silica mesoporous microsphere for the detection of glucose, *Analytica Chimica Acta* 840 (2014) 68-74.

[40] P. C. Ray, A. Fortner, G. K. Darbha, Gold nanoparticle based FRET assay for the detection of DNA cleavage, *J. Phys. Chem. B* 110 (2006) 20745-20748.

[41] J. Griffin, A. K. Singh, D. Senapati, P. Rhodes, K. Mitchell, B. Robinson, E. Yu, P. C. Ray, Size- and distance-dependent nanoparticle surface-energy transfer (NSET) method for selective sensing of hepatitis C virus RNA. *Chem.-Eur. J.* 15 (2009) 342-351.

[42] M. Li, S.K. Cushing, Q.Y. Wang, X.D. Shi, L.A. Hornak, N.Q. Wu, Size-dependent energy transfer between CdSe/ZnS quantum dots and gold nanoparticles, *J. Phys. Chem. Lett.* 2 (2011) 2125-2129.

[43] J. L. Wang, B. A. Cunningh, G. M. Edelman, Unusual fragments in the subunit structure of concanavalin A, *Proc. Natl. Acad. Sci. U.S.A.* 68 (1971) 1130.

[44] G. H. Mckenzie, W. H. Sawyer, L. W. Nichol, Molecular weight and stability of concanavalin A, *Biochim. Biophys. Acta* 263 (1972) 283.

[45] Z. H. Shen, M. C. Huang, C. D. Xiao, Y. Zhang, X. Q. Zeng, and P. G. Wang, Nonlabeled quartz crystal microbalance biosensor for bacterial detection using carbohydrate and lectin recognitions, *Anal. Chem.* 79 (2007) 2312-2319.

Captions:

Scheme 1 (A) Illustration of the fluorescence "turn off-on" biosensor for Con A detection based on CM-CHIT-QDs and Au NPs. (B) Chemical structure of the major unit of CM-CHIT.

Fig. 1 The UV-Vis absorption and fluorescence emission spectra of $CuInS_2$ QDs (dash line) and CM-CHIT-QDs (solid line).

Fig. 2 The FT-IR spectra of the $CuInS_2$ QDs (red curve) and CM-CHIT-QDs (green curve).

Fig. 3 (A) The RLS spectra of CM-CHIT-QDs/Au NPs/Con A (a), CM-CHIT-QDs/Au NPs (b), CM-CHIT-QDs (c), Con A (d) and Au NPs (e) system. (B) The CD spectra of Con A before and after the conjugation of CM-CHIT-QDs/Au NPs. The final concentration of CM-CHIT-QDs was 3.14×10^{-5} mol·L^{-1} QDs to 3.85 g·L^{-1} CM-CHIT. The concentration of Au NPs and Con A are 3.2 nM and 192.5 nM, respectively.

Fig. 4 The fluorescence spectra of CM-CHIT-QDs in the presence of different concentration of Au NPs (from 0 to 3.2 nmol·L^{-1}). Inset: The fluorescence quenching ratios I/I_0 versus the concentration of Au NPs. I and I_0 are the fluorescence intensity of CM-CHIT-QDs in the presence and absence of Au NPs. All the RSD values were less than 2.0% (mean of three replicates).

Fig. 5 (A) The effect of the CM-CHIT concentration on the fluorescence of CM-CHIT-QDs. (B)

The effect of pH on the fluorescence intensity of CM-CHIT-QDs/Au NPs system in the absence and presence of Con A. (C) The effect of salt concentration on the fluorescence intensity of CM-CHIT-QDs/Au NPs system in the absence and presence of Con A. (D) The effect of incubation time on the fluorescence intensity of CM-CHIT-QDs in the presence of Au NPs. (E) The effect of incubation time on the fluorescence intensity of CM-CHIT-QDs/Au NPs in the presence of Con A. I and I_0 are the fluorescence intensity of CM-CHIT-QDs/Au NPs in the presence and absence of Au NPs. The final concentration of CM-CHIT-QDs was 3.14×10^{-5} mol·L^{-1} QDs to 3.85 g·L^{-1} CM-CHIT. The concentration of Au NPs and Con A are 3.2 nM and 192.5 nM, respectively. All the RSD values were less than 2.0% (mean of three replicates).

Fig. 6 (A) The fluorescence spectra of CM-CHIT-QDs/Au NPs system in the presence of different concentrations of Con A (0, 0.2, 27.5, 55, 82.5, 110, 137.5, 165, 192.5, 220, 247.5, 275 and 302.5 nmol·L^{-1}, respectively). Inset: The relationship between the fluorescence intensity ratio I/I_0 and the concentration of Con A (from 0.2 to192.5 nmol·L^{-1}). I and I_0 were the fluorescence intensity of CM-CHIT-QDs/Au NPs system in the presence and absence of Con A, respectively. (B) The fluorescence spectra of CM-CHIT-QDs system in the presence of different concentrations of Con A (0, 2.5, 10, 15, 20, 25, 30, 35, 40, 45, 50, 60, 70, 80 and 90 nmol·L^{-1}, respectively). Inset: The relationship between the fluorescence intensity ratio I/I_0 and the concentration of Con A (from 2.5 to 45 nmol·L^{-1}). I and I_0 were the fluorescence intensity of CM-CHIT-QDs system in the presence and absence of Con A, respectively. All the RSD values were less than 2.0% (mean of three replicates).

Fig. 7 (A) The illustration of the fluorescence nanosensor for the determination of Con A based on chitosan capped $CuInS_2$ quantum dots. (B) Chemical structure of the major unit of CM-CHIT.

Table 1 The interference of coexisting substances on the determination of Con A (1 nmol·L^{-1})

Table 2 Results of Con A determination in fetal bovine serum samples

Figures:

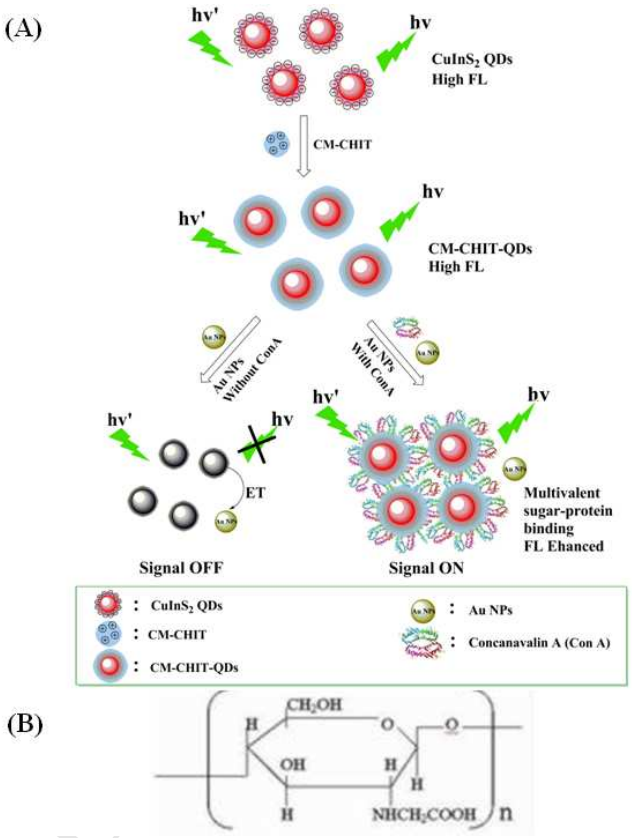

Scheme 1

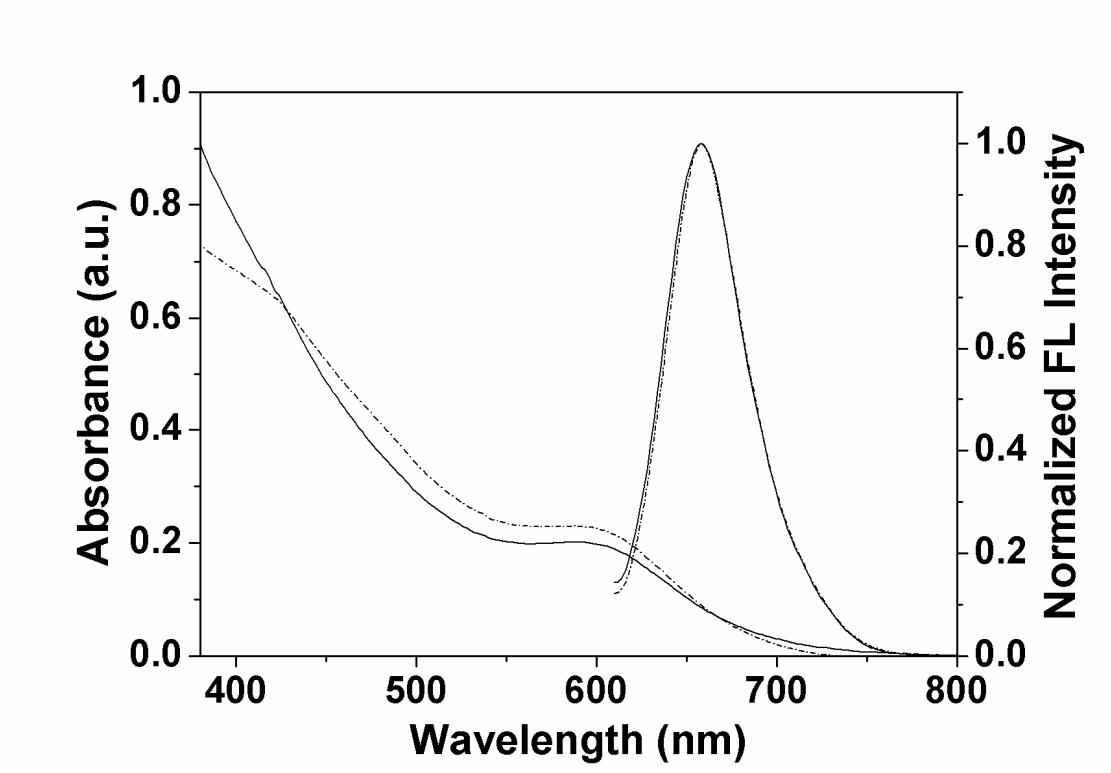

Fig. 1

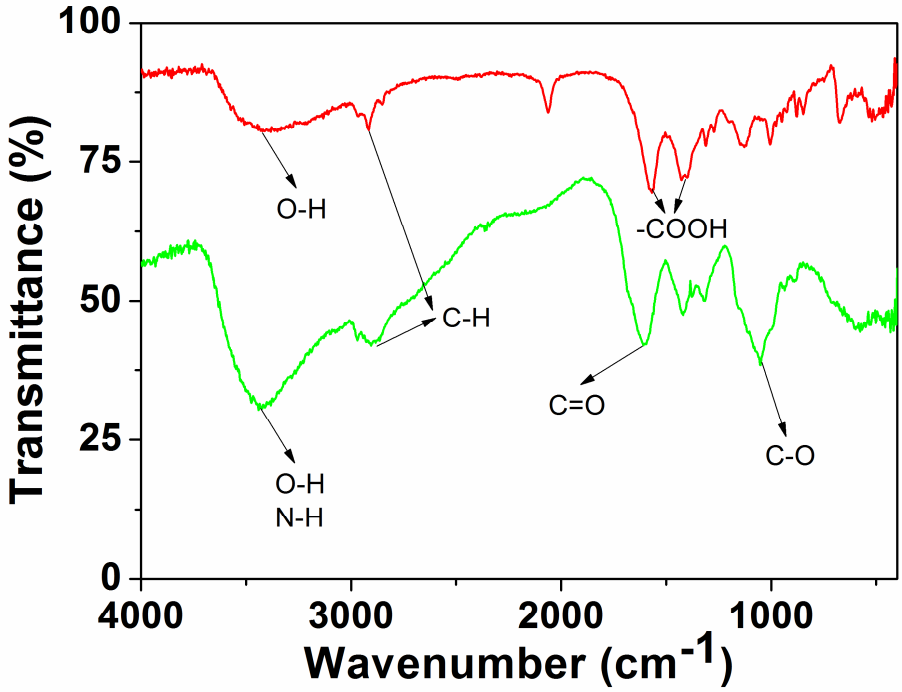

Fig. 2

(A) **(B)**

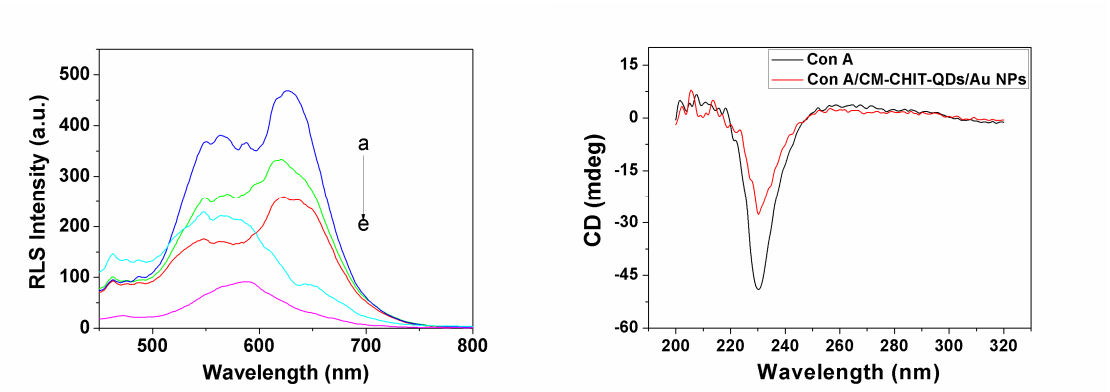

Fig. 3

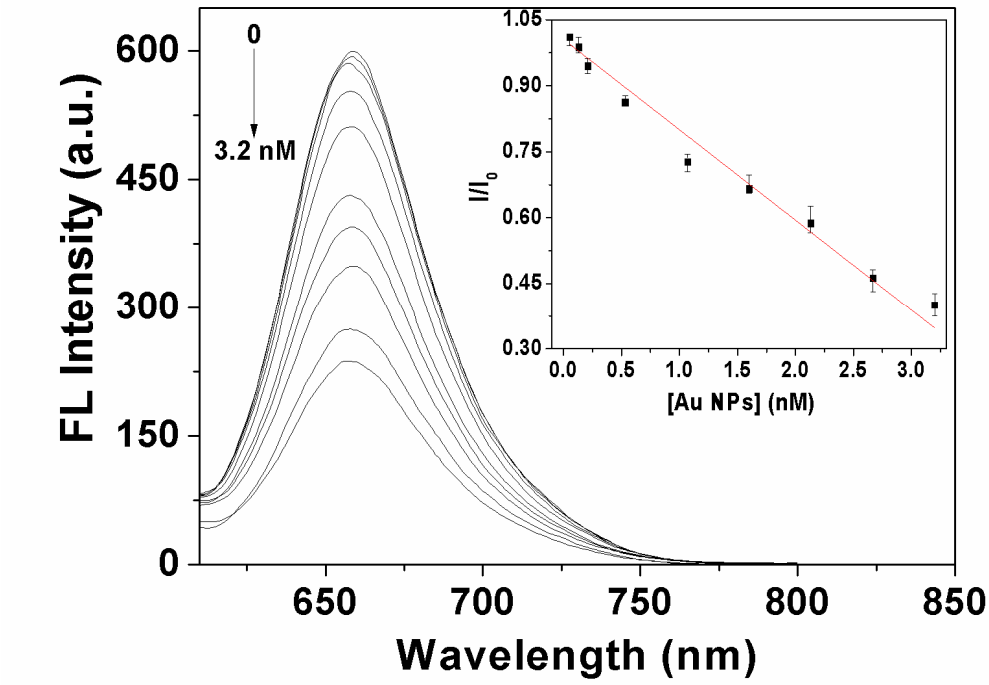

Fig. 4

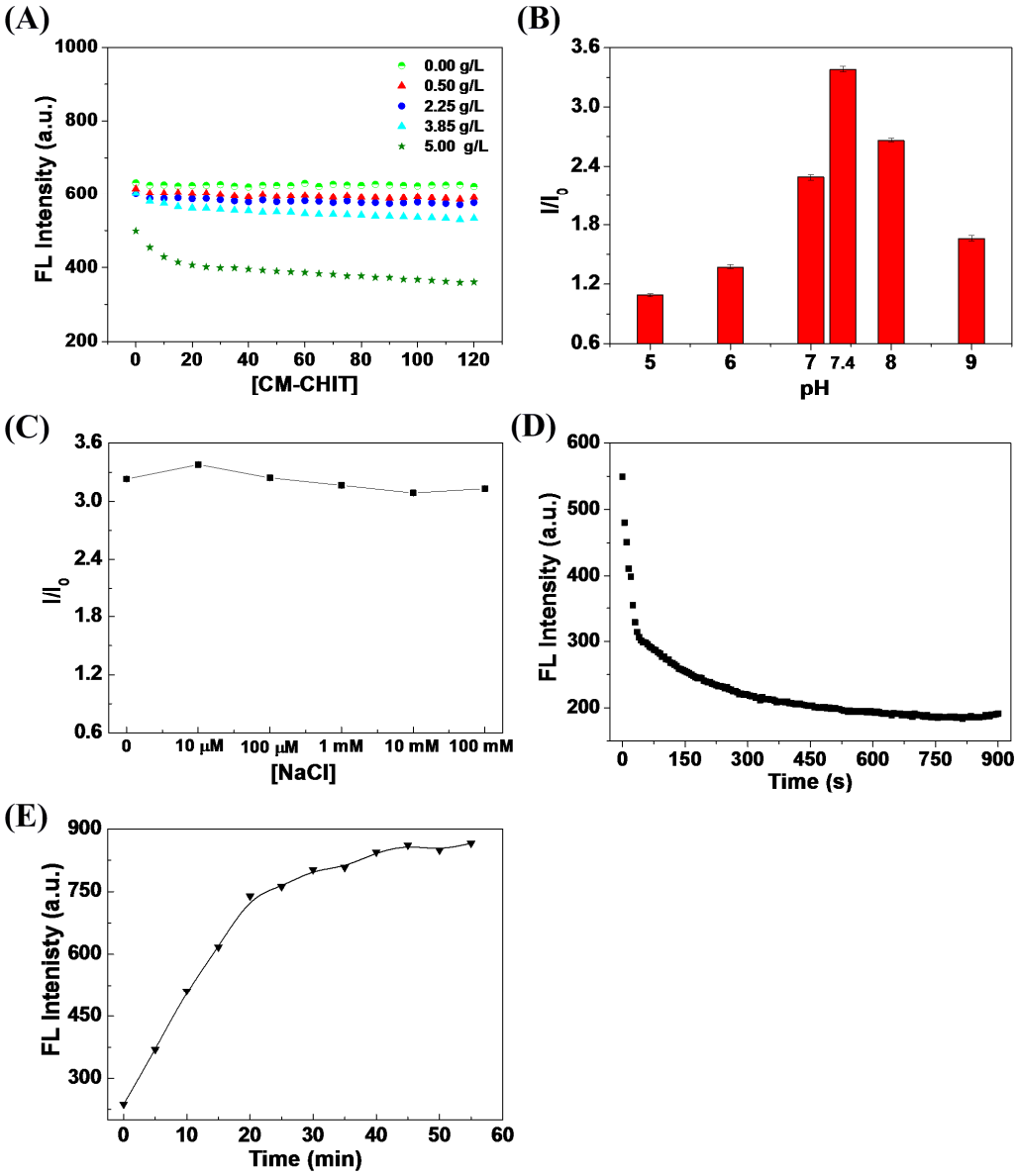
(A)
FL Intensity (a.u.)
[CM-CHIT]
0.00 g/L
0.50 g/L
2.25 g/L
3.85 g/L
5.00 g/L
(B)
I/I0
pH
(C)
I/I0
[NaCl]
0
10 μM
100 μM
1 mM
10 mM
100 mM
(D)
FL Intensity (a.u.)
Time (s)
(E)
FL Intenisty (a.u.)
Time (min)

Fig. 5

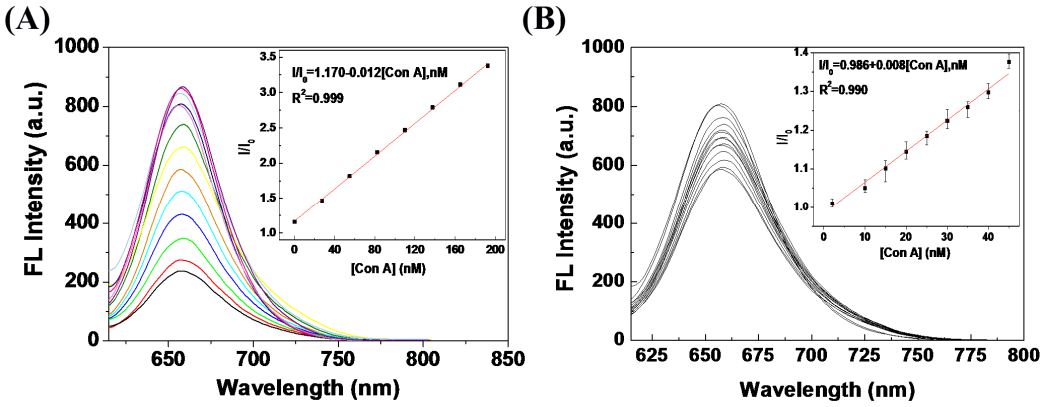

Fig. 6

(A)

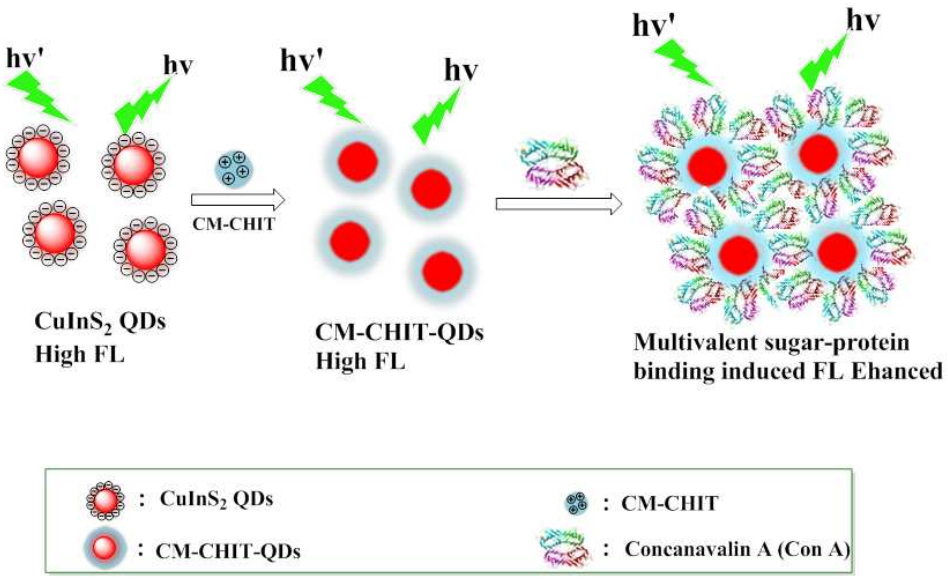

(B)

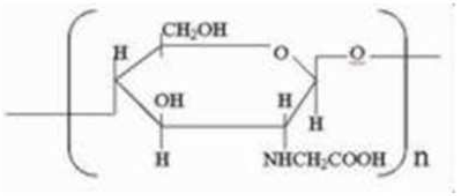

Fig. 7

T**able 1** The interference of coexisting substances on the determination of Con A (1 nmol·L^{-1})

Coexisting substance	Tolerable concentration	Molar ratio	ΔI/I (%)
Na^+	1 μmol·L^{-1}	10^3	1.97
K^+	1 μmol·L^{-1}	10^3	0.75
Cl^-	1 μmol·L^{-1}	10^3	-4.64
NO^{3-}	1 μmol·L^{-1}	10^3	-1.37
SO_4^{2-}	1 μmol·L^{-1}	10^3	4.98
Glucose	500 nmol·L^{-1}	10^2	2.78
Fructose	500 nmol·L^{-1}	10^2	2.28
Galactose	500 nmol·L^{-1}	10^2	3.16
BSA	10 μg·mL^{-1}	10^2	3.00
HSA	10 μg·mL^{-1}	10^2	0.33
Hep	10 μg·mL^{-1}	10^2	1.26
Lyz	100 nmol·L^{-1}	10^2	0.81

$\Delta I = I_0 - I$, where I and I_0 are the fluorescence intensities of the CM-CHIT-QDs/Au NPs/Con A system in the presence and absence of interfering species. For Con A, 1 nmol·L^{-1}= 0.1 μg·mL^{-1}.

Table 2 Results of Con A determination in fetal bovine serum samples

Sample	Added (nM)	Found (nM)	Recovery (%)	RSD (n=3, %)
1	0.50	0.49	98.00	3.12
2	1.00	1.01	101.0	2.22
3	1.50	1.46	97.33	1.69

Highlights:

► A label-free near-infrared fluorescence “turn off-on” biosensor for detection of lectin was established.

► The highly sensitive biosensor was based on the inner filter effect of Au NPs on CM-CHIT-QDs.

► Lectin could bind exclusively to CM-CHIT-QDs via multivalent carbohydrate-protein interactions, and “turn on” the fluorescence of CM-CHIT-QDs.

► The biosensor sensor showed good selectivity for the detection of lectin with a low detection limit of 0.07 nM.